



Structural, Optical and Magnetic Investigation of Ni, Co and Mn doped SnO₂ Nano particles Synthesized by Chemical Co-precipitation.

N. Makram

Nano-material Lab., Physics Depart., faculty of Science, al-Azhar University, Cairo, Egypt

Email address: nahedmkrm74@gmail.com

Abstract

Pure and transition metal doped nano-crystalline Sn_{1-x}TM_xO₂ (x = 0.0, 0.05, TM = Ni, Co and Mn) were synthesized in aqueous solution by chemical Co-precipitation technique. X-ray diffraction (XRD), high resolution transmission electron microscope (HR-TEM), electron diffraction, UV – visible absorption spectroscopy and room temperature magnetization measurements were performed to investigate the structural and microstructural, morphology, optical and magnetic properties of pure and doped samples. The structure calculations revealed that Co and Ni atoms have been incorporated in the SnO₂ host lattice. For Mn, the XRD analysis detected that SnO phase was formed instead during the synthesis process. HRTEM and XRD studies indicated that the particle size is in the range of quantum dot size except for Mn. For optical measurement, the quantum confinement effect was suggested to be the dominant reason for the great increase of the optical bandgap with respect to the bulk material. Magnetization measurements revealed that all doped samples were ferromagnetic in nature. Well defined strong hysteresis loop was detected for Co doped SnO₂ nanoparticles. It was suggested that the ferromagnetism is intrinsic in origin. It is not due to ferromagnetic metal clusters nor due to the presence of additional ferromagnetic phases. The strong ferromagnetic signal especially for Co doped SnO₂ makes it a candidate for spintronic applications.

Keywords

Doped SnO₂ nanoparticle - chemical co-precipitation - HRTEM - ferromagnetism.

Council for Innovative Research

Peer Review Research Publishing System

Journal: JOURNAL OF ADVANCES IN PHYSICS

Vol. 11, No. 5

www.cirjap.com, japeditor@gmail.com



1. Introduction

The study of diluted magnetic semiconductor (DMS) is being carried out since last few decades. Apart from the present day applications in the field of spintronics, they are interesting to the physics community due to the rich variety of phenomena and physics they exhibit [1-4]. Preparation of single phase diluted magnetic semiconductor, devoid of any secondary phases or metallic clusters, is a big challenge. Even if the material is a single phase, the magnetism in these systems has always been controversial and the debate on the origin and the mechanism of ferromagnetism is far from over [5].

Many reports are available on room temperature ferromagnetism (RTFM) in various transition metal doped oxides, but no reports have clearly explained the origin of ferromagnetism. It may be intrinsic or due to the presence of hidden secondary phases of ferromagnetic metal clusters or their ferromagnetic oxides [6-8].

Recently, the RTFM has been actively investigated in the transition metal incorporated TiO_2 [9-13], ZnO [14-18], CuO [19] etc. These oxides doped with TM is characterized by the large $sp-d$ exchange interaction between the magnetic ions and the band electrons [20]. In fact, maintaining sufficiently high optical transparency in these oxides (optical gap width > 3 eV), gives rise for new applications with these semiconductors.

Among the other known metal oxide semiconductors, SnO_2 is a very interesting oxide material with a wide band gap. Its higher optical transparency, chemical stability, metal like conductivity and easy doping make it a very attractive material for optoelectronic devices, catalysis and gas sensing applications. In the nano-scale form TM-doped SnO_2 is reported to demonstrate more interesting structural and magnetic properties [21].

In this work, we report ferromagnetism in chemically synthesized, single phase, Co, Ni and Mn doped tin oxide nanoparticles. The structural, microstructural and optical properties of the prepared

$\text{Sn}_{1-x}\text{TM}_x\text{O}_2$ have also been investigated.

2. Experimental Details

$\text{Sn}_{1-x}\text{TM}_x\text{O}_2$ (TM = Ni, Co and Mn) and ($x = 0, 0.05$) nanoparticle system was synthesized by the Co-precipitation method. All the reagents used are of analytical grade (Sigma Aldrich 99.9 %) and handled without further purification. Aqueous solutions of precursors $\text{SnCl}_2 \cdot 2\text{H}_2\text{O}$, $\text{CoCl}_2 \cdot 6\text{H}_2\text{O}$, $\text{NiCl}_2 \cdot 6\text{H}_2\text{O}$ and $\text{C}_4\text{H}_6\text{MnO}_4$ (1M) were separately prepared in distilled water as per stoichiometric ratio and stirred for 4 hours. Sodium hydroxide (NaOH) was added drop wise under constant stirring to maintain the chemical homogeneity until the white precipitates were obtained. The pH value was controlled to equal 7. After 30 minutes of stirring the precipitate was washed several times with de-ionized water to remove chlorine and other ionic impurities formed during the synthesis process. The washed precipitates were filtered out separately and dried in an oven at 50°C for 24 hours. The obtained product were grounded, collected carefully and then annealed at 400°C for 2 hours to obtain ($\text{Sn}_{1-x}\text{TM}_x\text{O}_2$) nanoparticle system. Structural investigations by XRD were carried out using $\text{Cu-K}\alpha$ radiation ($\lambda = 1.5418 \text{ \AA}$) using a Philips X'Pert MPP diffractometer with goniometer type Pw 3050/10. A transmission electron microscope (TEM) model Tecnai G20, Super twin, double tilt with applied voltage: 200 KV and magnification range up to 1,000,000 x and Gun type LaB 6 Gun, was used to identify the microstructure and surface morphology. The magnetization as a function of the applied magnetic field was measured at room temperature by employing a vibrating sample magnetometer (VSM) model Lake Shore 7410 with an applied field of 301T. An optical absorption study of the prepared system was also performed using a spectrophotometer model JASCO – V-670.

3. Results and Discussion

3.1. Structural and Microstructural Analysis

3.1.1. XRD analysis

The x-ray diffraction patterns of $\text{Sn}_{1-x}\text{TM}_x\text{O}_2$ samples are shown in Fig. (1). Applying the search match program, no diffraction lines were found for Sn, Ni, Co or Mn elements. Only one pure phase of SnO_2 was detected for pure SnO_2 and Ni doped sample according to the specific ICDD card number (04-008-8133) confirming the formation of tetragonal structure with space group $P4_2/mnm$ and lattice parameter $a = 4.7421 \text{ \AA}$ and $c = 3.1901 \text{ \AA}$. Adding the Co atom into SnO_2 enhances the formation of a minor phase of SnO together with the major phase as shown in Fig. (1-c) and table (2). For $\text{Sn}_{0.95}\text{Mn}_{0.05}\text{O}_2$ sample only one major phase of SnO was formed during the synthesis process as given in table (2). The specific ICDD card number (04-008-7670) confirming the formation of tetragonal structure for the SnO Phase with space group $P4/nmm$ and lattice parameter $a = 3.8036 \text{ \AA}$ and $c = 4.8385 \text{ \AA}$. This SnO phase is characterized by sharp diffraction lines i.e. more ordering crystalline structure as shown in the XRD pattern of Fig. (1-d).

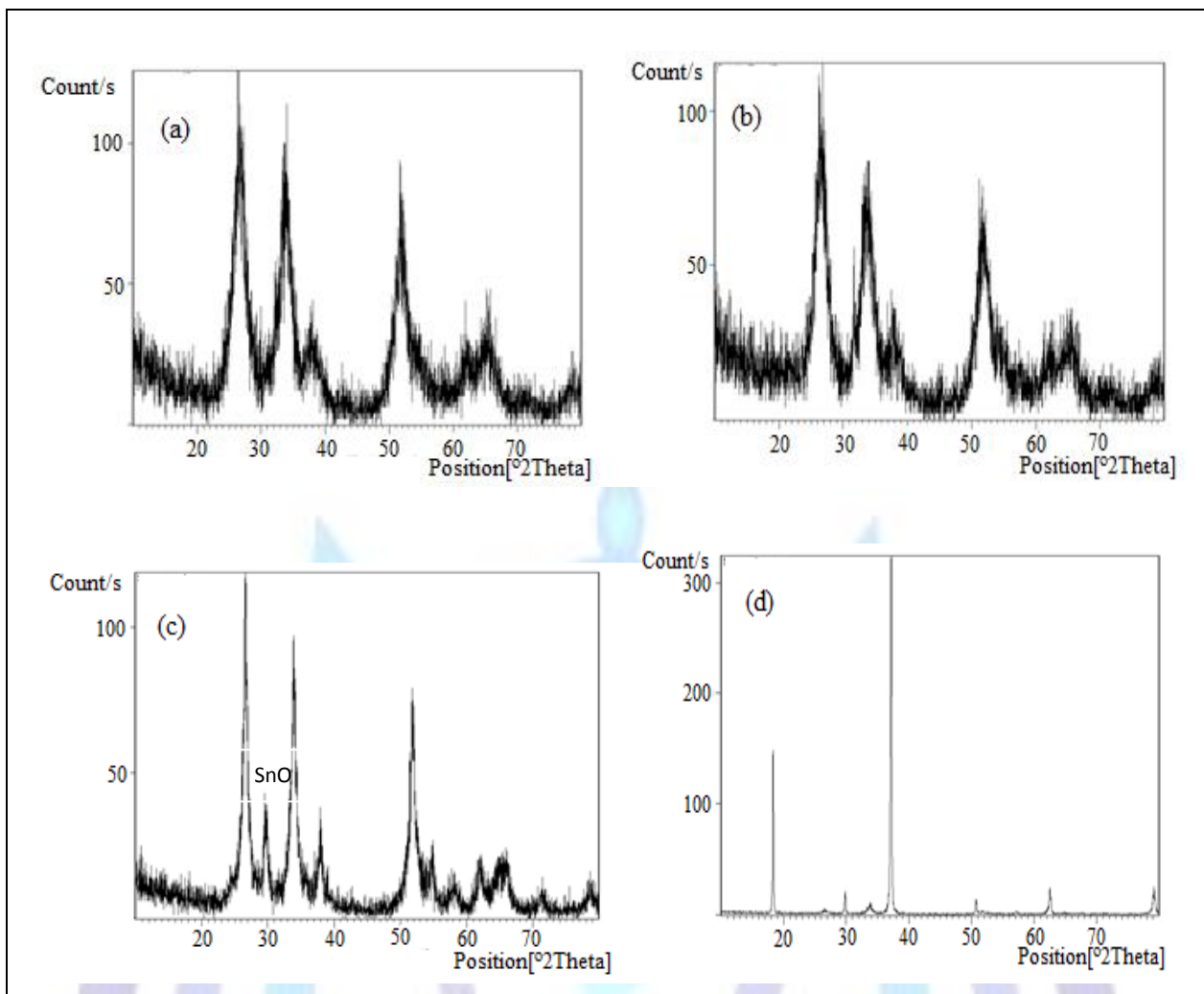


Fig.(1, a - d): The X–ray diffraction patterns for the prepared nanoparticlesystem(a) SnO_2 , (b) $\text{Sn}_{0.95}\text{Ni}_{0.05}\text{O}_2$ (c) $\text{Sn}_{0.95}\text{Co}_{0.05}\text{O}_2$ and (d) $\text{Sn}_{0.95}\text{Mn}_{0.05}\text{O}_2$.

Applying the Win-fit program the resulting apparent crystallite size D_β (nm) and D_F (nm) and root mean square strain $\langle \epsilon \rangle$ from single line analysis are given in table (1,2) . The data revealed that the size of the quantum dots of SnO_2 (2.7-2.9 nm) increases to (4.6-5.2 nm) as Ni was added. For Co and Mn bigger crystallite size were detected (13.9-14.4 nm and 26.2-28.2 nm respectively).

Table (1): Apparent crystallite size D_β (nm) & D_F (nm) from single line analysis for the prepared SnO_2 and $\text{Sn}_{0.95}\text{Ni}_{0.05}\text{O}_2$ nanoparticle samples.

SnO_2			$\text{Sn}_{0.95}\text{Ni}_{0.05}\text{O}_2$		
single line analysis of SnO_2 phase			single line analysis of SnO_2 phase		
hkl	D_β (nm)	D_F (nm)	hkl	D_β (nm)	D_F (nm)
110	2.4	2.6	110	3.9	4.4
101	1.8	2.1	101	4.1	4.6
111	1.5	1.8	200	4.9	5.4
211	5.3	5.4	112	5.7	6.2
221	3.2	3.5			
301	2.2	2.4			
Average	2.7	2.9	Average	4.6	5.2

**Table (2): Apparent crystallite size D_{β} (nm) & D_F (nm) for single line analysis for the prepared $\text{Sn}_{0.95}\text{Co}_{0.05}\text{O}_2$ and $\text{Sn}_{0.95}\text{Mn}_{0.05}\text{O}_2$ nanoparticle samples.**

$\text{Sn}_{0.95}\text{Co}_{0.05}\text{O}_2$			$\text{Sn}_{0.95}\text{Co}_{0.05}\text{O}_2$			$\text{Sn}_{0.95}\text{Mn}_{0.05}\text{O}_2$		
single line analysis of SnO_2 phase			single line analysis of SnO phase			single line analysis of SnO phase		
hkl	D_{β} (nm)	D_F (nm)	hkl	D_{β} (nm)	D_F (nm)	hkl	D_{β} (nm)	D_F (nm)
110	14.8	15.1	101	13.6	13.9	001	30.6	31.4
101	13.8	14.1				101	26.9	28.7
200	15.1	15.3				002	27.8	32.0
211	13.9	14.2				112	20.8	21.9
220	14.1	14.5				103	25.1	26.9
002	17.7	18.9				Average	26.2	28.2
310	12.1	12.3						
301	14.1	14.3						
202	10.1	11.4						
Average	13.9	14.4						

3.1.2. HRTEM Analysis

The HRTEM images for the system under study are shown in Fig. (2, a - d). It is clear from figures that spherical shaped nanoparticles have been formed in the un-doped and transition metal ion doped SnO_2 . The size, estimated from individual nanocrystals for SnO_2 and $\text{Sn}_{0.95}\text{Ni}_{0.05}\text{O}_2$ is in the quantum dot range 3.37- 5.85 and 3.31 – 4.97 nm respectively. For Co and Mn doped SnO_2 , the crystallite size increases to 16.8- 18.3 and 28.2 – 30.4 nm respectively. These values are in good agreement with those determined from the XRD analysis. Similar results for the particle size in undoped and SnO_2 doped samples were also reported [22-24].

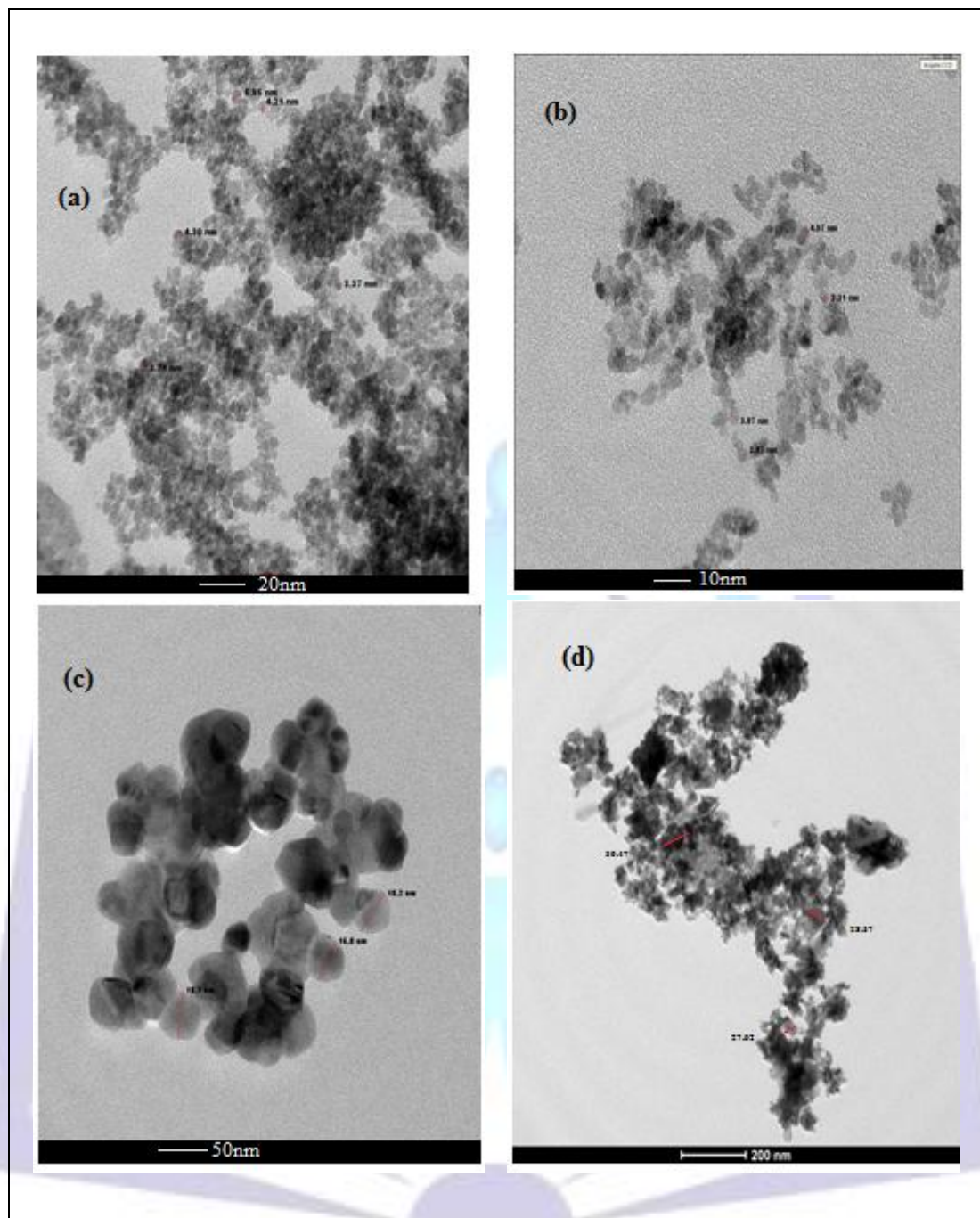


Fig. (2, a –d): The HRTEM images for the prepared nanoparticle system (a) SnO_2 , (b) $\text{Sn}_{0.95}\text{Ni}_{0.05}\text{O}_2$,
(c) $\text{Sn}_{0.95}\text{Co}_{0.05}\text{O}_2$ and(d) $\text{Sn}_{0.95}\text{Mn}_{0.05}\text{O}_2$.

The selected area electron diffraction (SAED) patterns of the samples under study are shown in Fig. (3, a - d) for the prepared SnO_2 , $\text{Sn}_{0.95}\text{Ni}_{0.05}\text{O}_2$, $\text{Sn}_{0.95}\text{Co}_{0.05}\text{O}_2$ and $\text{Sn}_{0.95}\text{Mn}_{0.05}\text{O}_2$. These patterns show that all crystalline rings can be indexed to a rutile type tetragonal crystal structure.

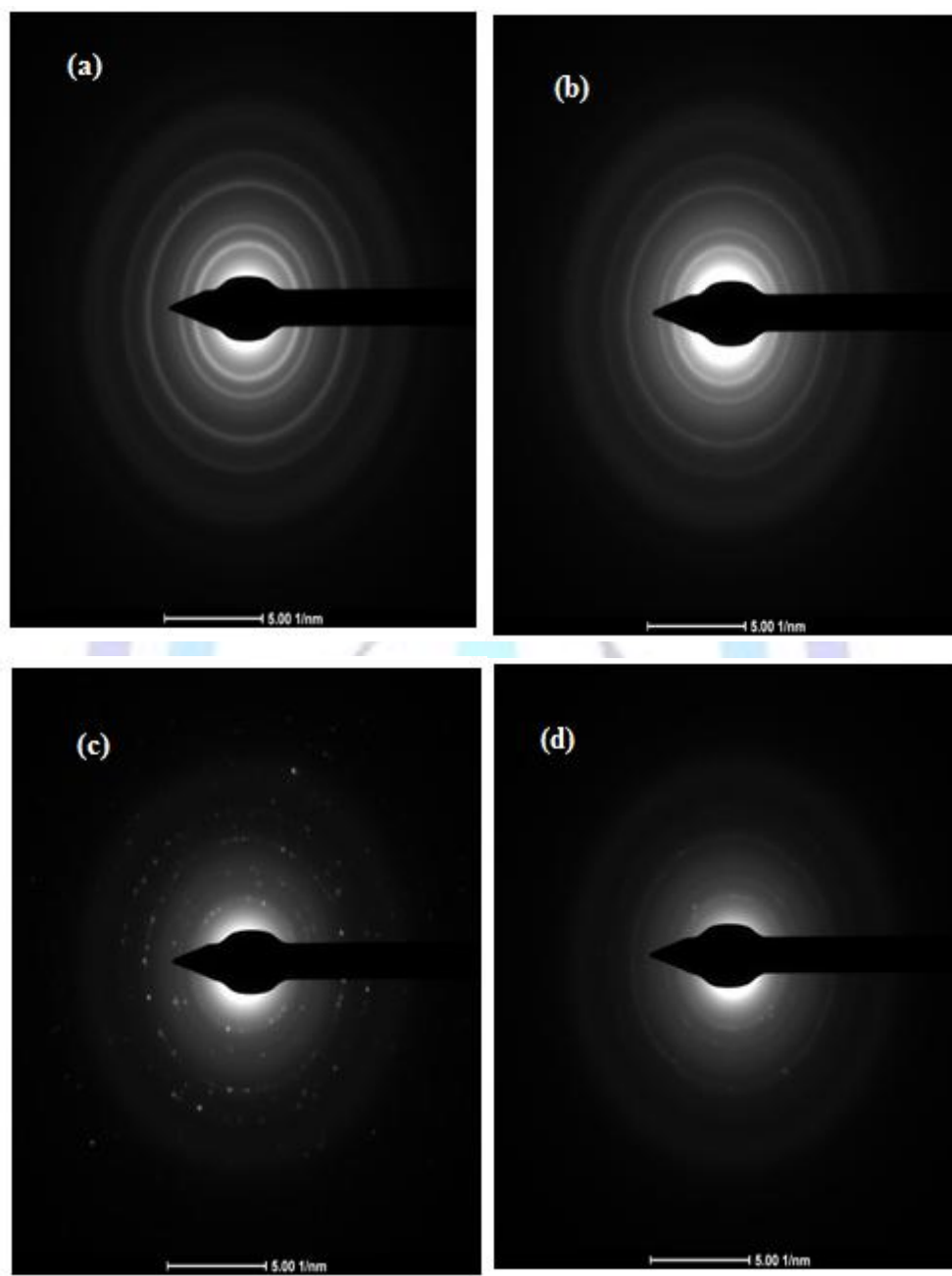


Fig. (3, a –d): The SAED patterns for the prepared nanoparticle systems

(a) SnO_2 , (b) $\text{Sn}_{0.95}\text{Ni}_{0.05}\text{O}_2$, (c) $\text{Sn}_{0.95}\text{Co}_{0.05}\text{O}_2$ and(d) $\text{Sn}_{0.95}\text{Mn}_{0.05}\text{O}_2$.

3.2. Magnetic studies

To probe the magnetic properties of ($\text{Sn}_{1-x}\text{TM}_x\text{O}_2$) nanoparticle system, where $x = 0$ and 0.05 and $\text{TM} = \text{Ni}, \text{Co}$ and Mn , the field dependent magnetization curves (M-H) taken at room temperature with applied magnetic field ranging from -15KG to 15KG were measured. As given in Fig. (4), it is clear that the undoped SnO_2 nanoparticles exhibit the diamagnetic behavior with a negative magnetic susceptibility. This may be due to the $4+$ valance state of Tin (Sn^{4+}) favouring $4d^{10}$ electronic configuration of Sn in SnO_2 and, hence, there is no unpaired d electrons in the materials for any kind of ferromagnetic ordering. Partial substitution of Ni and Mn ions for Sn transformed it from diamagnetic state to a weak ferromagnetic ordering state with a very narrow hysteresis loop and a small value of corecivity (Hci) as shown in table (3).

The room temperature magnetization of Co-doped SnO_2 showed significant hysteresis at room temperature, reflecting a good ferromagnetic ordered state (Fig. 4). The ferromagnetic behavior of Co-doped SnO_2 shows a hysteresis loop at low magnetic field followed by a linear increase in magnetization at higher fields. A high corecivity (Hci) of $\sim 544.29\text{G}$ was recorded. This type of linear behavior might be attributed to the magnetic moment associated with the conduction electrons[25]. It has been suggested that room- temperature ferromagnetism results from the magnetic coupling between oxygen vacancy (V_o) centers at the surface of the nanoparticles[26-28].

The origin of ferromagnetism in Ni, Co and Mn doped SnO₂ could be attributed to oxygen deficiency, formation of TM related secondary phases and metallic TM clusters. No magnetic phases of TMO₂ and no metallic TM clusters were detected by XRD analysis. Hence, one can conclude that the ferromagnetic character observed for the TM doped SnO₂ is not due to any additional magnetic phase but it is only caused by TM doping. The appearance of ferromagnetism with Mn as a dopant can be attributed to the presence of secondary phases, since nearly all of the possible Mn – based binary and ternary oxide candidates are anti-ferromagnetic with a Néel temperature far below room temperature [29]. The XRD analysis and electron diffraction have not revealed any Mn – O phases for the present case. This ferromagnetism may be a result of the interaction of the Mn d orbital with the sp orbital of SnO₂. K. Gopinadhan et.al.have reported according to structural and optical investigation that Sn_{1-x}Mn_xO₂ forms a random alloy as Mn ions are incorporated irregularly in SnO₂ lattice [30].

Some Mn ion separations into the SnO₂ lattice may be less than others; hence an anti-ferromagnetism may occur locally reducing therefore the overall magnetization. This may give account for the low value of coercivity (H_{ci}) measured for the present study (59.28G). Similar interpretation can be also given for Ni doped SnO₂, because if Ni atom pairs come closer sufficiently, the super-exchange interaction is expected between the TM atoms. This may lead to an anti-ferromagnetic type interaction leading to the moderate values of M_s and M_r. Previous results reported similar data for Ni concentration higher than X = 0.03 [21]. It is likely that, the room temperature ferromagnetism in Ni, Co and Mn doped SnO₂ samples is intrinsic to the material.

As seen from Fig.(4) and table (3) The ferromagnetic signal is greatly enhanced for Co doped SnO₂ as a strong well defined hysteresis loop was detected. The highest saturation magnetic moment of 56.63×10⁻³ (emu/g) and coercive field of 544.29 G may be due to the substitution of Co²⁺ with Sn⁴⁺ which favours an increase of oxygen vacancies available for electron trapping and hence increase in saturation magnetic moment. Such substitution may increase the local hole concentration, hence the local density of states at the Fermi level giving rise to the double exchange interaction, consequently an increase of ferromagnetism.

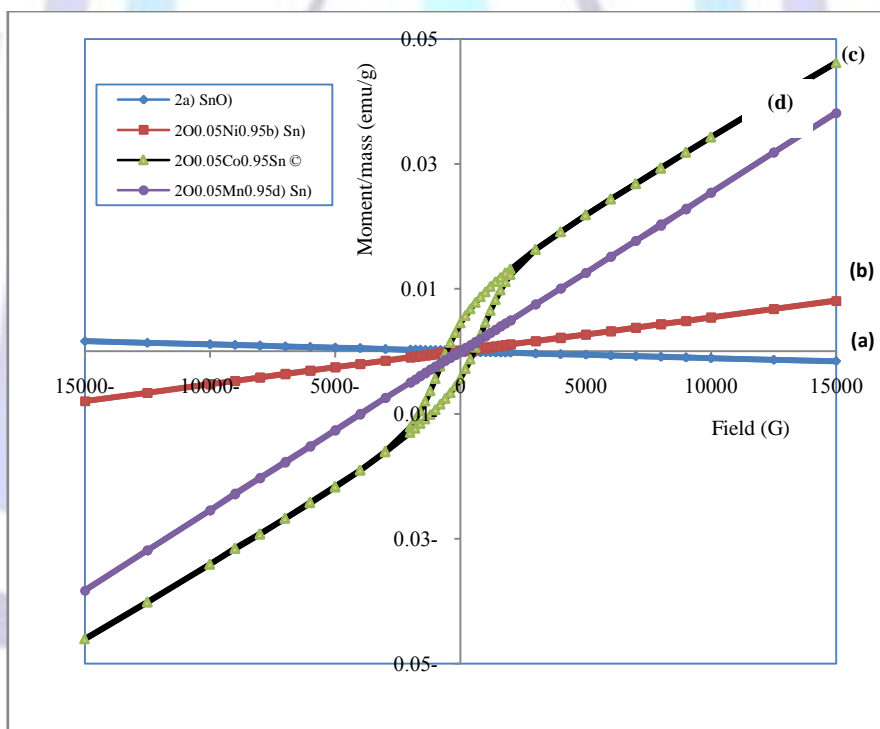


Fig. (4) The hysteresis loops of the prepared Sn_{1-x}TM_xO₂ system.

Table (3): The magnetic parameter M_s, M_r, M_r/M_s and H_{ci} for the nanoparticlesystems under study.

Sample	M _s (emu/g)	M _r (emu/g)	M _r /M _s	H _{ci} (G)
Sn _{0.95} Ni _{0.5} O ₂	10.46 × 10 ⁻³	95.217 × 10 ⁻⁶	9.1029 × 10 ⁻³	212.21
Sn _{0.95} Co _{0.5} O ₂	56.629 × 10 ⁻³	4.428 × 10 ⁻³	7.8193 × 10 ⁻³	544.29
Sn _{0.95} Mn _{0.5} O ₂	49.756 × 10 ⁻³	130.33 × 10 ⁻⁶	2.61938 × 10 ⁻³	59.287

3.3. Optical Properties

Absorption spectroscopy was used to explore the energy band gap changes brought about by the presence of Ni, Co and Mn dopant in SnO₂nanocrystallite. The absorption spectra of pure SnO₂ and TM doped SnO₂ are given in Fig. (5).

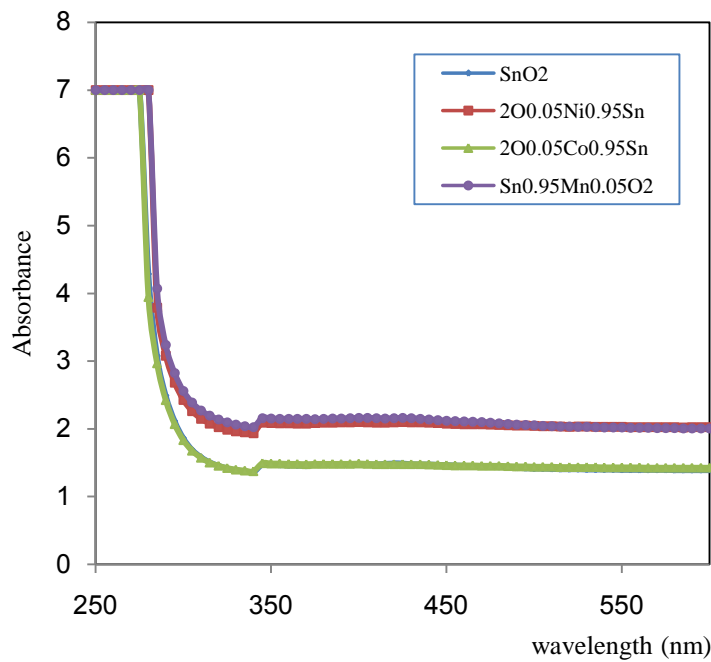
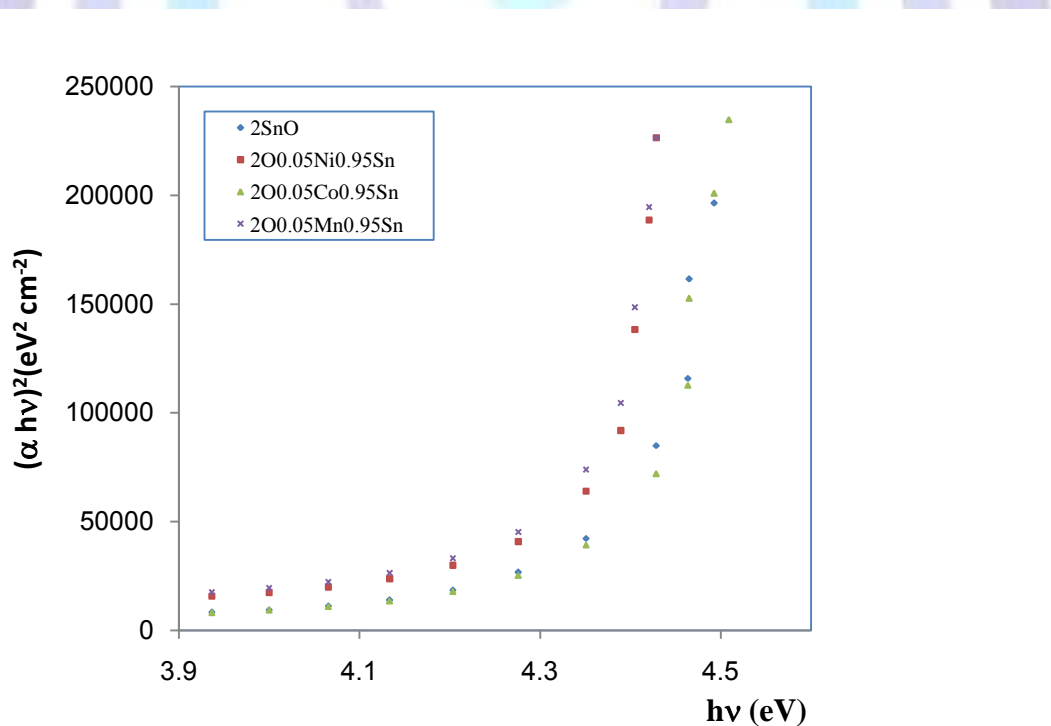


Fig. (5): Optical absorbance spectra of the prepared Sn_{1-x}TM_xO₂ Nanoparticle system.

The band gap width (E_g) was calculated according to Tauc's relation[31]. $\alpha h\nu = A (h\nu - E_g)^n$ (1)

Where α is the absorption coefficient, A is a constant and $n = \frac{1}{2}$ for direct band gap transition. E_g is estimated from the extrapolation of the linear portion of the plot $(\alpha h\nu)^2$ Vs. $h\nu$ as shown in Fig. (6). Values of E_g of the four samples are displayed in table (4) together with the particle size detected by XRD measurements.



(Fig.6) : Tauc's plots of the prepared Sn_{1-x}TM_xO₂ nanoparticle system.



The published E_g value of bulk SnO_2 is 3.6 eV[32]. The high E_g value given in table (4) can be attributed to quantum size effects in nano particles in accordance to the relation[33, 34].

$$E_g = E_{g_b} + \frac{\hbar^2 \pi^2}{2 \mu r^2} - Ry^* \quad (2)$$

where E_{g_b} is the energy band gap of the bulk, r is the particle radius, μ is the reduced mass and Ry^* is the Rydberg's energy. It could be suggested that the major reason for the blue shift in E_g for the nano-material is due to strong quantum confinement effects. As given in table (4) the prepared quantum dots SnO_2 has a high value of $E_g \sim (4.36\text{eV})$. A value of 3.76 eV was reported for SnO_2 with nano-size of ~ 26 nm prepared by mechanochemical processing[35], while a value of 4.07 eV was published for SnO_2 with average crystallite size in the range 4.78 nm stabilized with polyethylene glycol [23].

The decrease in the band gap energy for Ni and Mn doped SnO_2 with respect to the undoped sample may be due to the accumulation of donor energy levels of TM ions in the actual band gap of SnO_2 .

The value of the band tail width E_0 extended into the forbidden gap is calculated according to Urbach relation[32].

$$\alpha = \alpha_0 \exp (hu)/E_0 \quad (3)$$

The values of E_0 extracted from Fig. (7) are given in table (4).

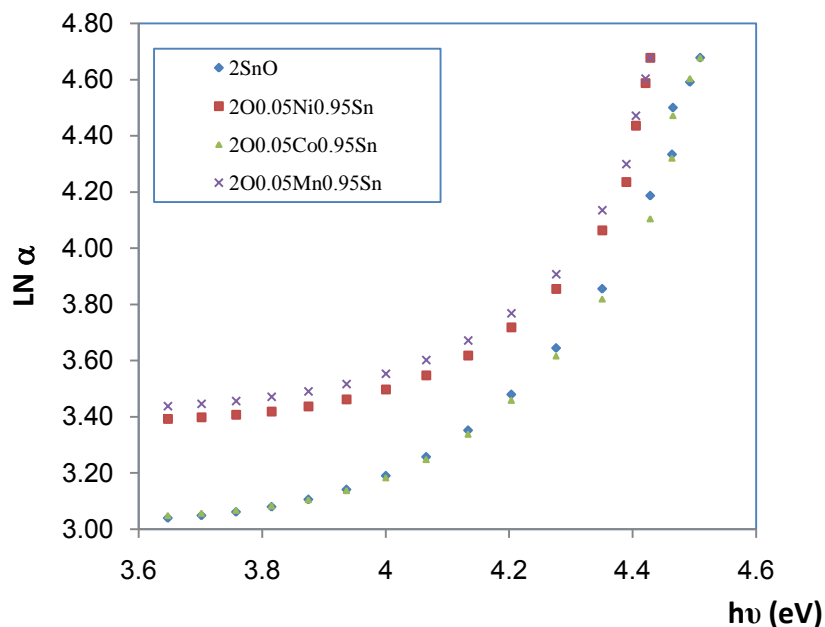


Fig. (7): The absorption coefficient of the prepared $\text{Sn}_{1-x}\text{TM}_x\text{O}_2$ nanoparticles system.

Table (4): The optical gap (E_g), the band tail width (E_0) and the particle size for the prepared $\text{Sn}_{1-x}\text{TM}_x\text{O}_2$ nanoparticle system.

sample	(E_g) (eV)	E_0 (eV)	Particle size (nm)
SnO_2	4.36	0.222	2.7
$\text{Sn}_{0.95}\text{Ni}_{0.05}\text{O}_2$	4.28	0.244	4.6
$\text{Sn}_{0.95}\text{Co}_{0.05}\text{O}_2$	4.35	0.215	13.9
$\text{Sn}_{0.95}\text{Mn}_{0.05}\text{O}_2$	4.28	0.251	26.2

In spite of the nanocrystalline structure, some localized states are formed at the band edges. It is clear that, the band tail is more extended into the forbidden gap for Ni and Mn doped SnO_2 in consistent with the narrowing of their energy band gap.

Conclusion

Room temperature ferromagnetism is exhibited by doped $\text{Sn}_{1-x}\text{TM}_x\text{O}_2$ ($x = 0,0.05$, TM = Ni, Co and Mn,) synthesized by chemical coprecipitation. XRD, electron diffraction in combination with magnetization study reveal that the



ferromagnetism is not due to any ferromagnetic phases. Optical measurements indicated a red shift in the absorption edge of Mn and Ni doped sample caused by the formation of donor energy levels inside the gap of SnO₂. The present study demonstrates that doping with 5 at % Co in SnO₂ nanomaterial gives rise to significant room temperature ferromagnetism ordering useful for spintronic applications.

Acknowledgment

The author is grateful to the Grants Commission of Al-Azharuniversity, Cairo - Egypt for supporting this work. The author is thankful to Nanotechnology Characterization Center (NCC) and Agriculture Research Center (ARC), Cairo University for extending the HRTEM and VSM facility.

Reference

- [1] J. K. Furdyna, *J. Appl. Phys.* R29 (1988), 64.
- [2] G. A. Prinz, *Science* 282(1998), 1660.
- [3] S. A. Wolf, D. D. Awschalom, R. A. Buhrman, J. M. Daughton, S. V. Molnar, M. L. Roukes, A. Y. Chtcheljanova and D. M. Treger, *Science* 294(2001), 1488.
- [4] David D. Awschalom and Michael E. Flatté, *Nat. Phys.* 3(2007), 153.
- [5] Sanghoon Lee, J.-H. Chung, Xinyu Liu, Jacek K. Furdyna, and Brian J. Kirby, *Mat. Today* 12(2009), 14.
- [6] C. Van Komen, A. Thurber, K.M. Reddy, J. Hays, A. Punnoose, *J. Appl. Phys.* 103 (2008), 07D141-3.
- [7] A. Punnoose, J. Hays, A. Thurber, M. H. Engelhard, R. K. Kukkadapu, C. Wang, V. Shutthanandan, *Phys. Rev. B* 72 (2005), 5402.
- [8] J.M.D. Coey, A.P. Douvalis, C.B. Fitzgerald, M. Venkatesan. *Appl. Phys. Lett.* 84 (2004), 1332-1334.
- [9] Y. Matsumoto, M. Murakami, T. Shono, T. Hasegawa, T. Fukumura, M. Kawasaki, P. Ahmet, T. Chikyow, S. Koshihara, and H. Koinuma, *Science* 291(2001), 854.
- [10] Y. Matsumoto, R. Takahashi, M. Murakami, T. Koida, X.-J. Fan, T. Hasegawa, T. Fukumura, M. Kawasaki, S.-Y. Koshihara, and H. Koinuma, *Jpn. J. Appl. Phys., Part 2*, 40(2001), L1204.
- [11] S. R. Shinde, S. B. Ogale, S. D. Sarma, J. R. Simpson, H. D. Drew, S. E. Lofland, C. Lanci, J. P. Buban, N. D. Browning, V. N. Kulkarni, J. Higgins, R. P. Sharma, R. L. Greene, and T. Venkatesan, *Phys. Rev. B* 67(2003), 115211.
- [12] K. A. Griffin, A. B. Pakhomov, C. M. Wang, S. M. Heald, and K. M. Krishnan, *Phys. Rev. Lett.* 94(2005), 157204.
- [13] J. W. Quilty, A. Shibata, J.-Y. Son, K. Takubo, T. Mizokawa, H. Toyosaki, T. Fukumura, and M. Kawasaki, *Phys. Rev. Lett.* 96(2006), 027202.
- [14] K. Ueda, H. Tabata, and T. Kawai, *Appl. Phys. Lett.* 79(2001), 988.
- [15] D. P. Norton, S. J. Pearton, A. F. Hebard, N. Theodoropoulou, L. A. Boatner, and R. G. Wilson, *Appl. Phys. Lett.* 82(2003), 239.
- [16] M. Venkatesan, C. B. Fitzgerald, J. G. Lunney, and J. M. D. Coey, *Phys. Rev. Lett.* 93(2004), 177206.
- [17] M. Kobayashi, Y. Ishida, J. I. Hwang, T. Mizokawa, A. Fujimori, K. Mamiya, J. Okamoto, Y. Takeda, T. Okane, Y. Saitoh, Y. Muramatsu, A. Tanaka, H. Saeki, H. Tabata, and T. Kawai, *Phys. Rev. B* 72(2005), 201201.
- [18] K. P. Bhatti, S. Kundu, S. Chaudhary, S. C. Kashyap, and D. K. Pandya, *J. Phys. D* 39(2006), 4909.
- [19] S. G. Yang, T. Li, B. X. Gu, Y. W. Du, H. Y. Sung, S. T. Hung, and C. Y. Wong, *Appl. Phys. Lett.* 83(2003), 3746.
- [20] Jasneet Kaur, Jaspreet Kaur, R.K. Kotnala, Vinay Gupta, Kuldeep Chand Verma, *Adv. Mat. Lett.* 3(6) (2012), 511-514.
- [21] Aditya Sharma, Mayora Varshney, Shalendra Kumar, K.D. Verma and Ravi Kumar, *Nanomater. Nanotechnol.*, 1(2011), 29-33.
- [22] S. Das, S. Kar and S. Choudhary, *J. Appl. Phys.* 99(2006), 114303.
- [23] K. Subramanyam, N. Sreelekha, G. Murali, D. Amaranatha Reddy, R.P. Vijayalakshmi, *Physica B* 454(2014), 86 – 92.
- [24] N. Iyavanaya, S. Radhakrishnan, C. Seka, M. Navaneethan, Y. Hayakawa, *Analyst* 138(2013), 2061-2067.
- [25] Tahir, N., Karim, A., Persson, K.A., Hussain, S. T., Cruz, A. G., Usman, M., Muhammad, N., Qiao, R., Yang, W., Chuang, Y. D. et al. *J. Phys. Chem. C*, 117(2013), 8968-8973.
- [26] Sundaresan, A., Bhargavi, R., Rangarajan, N., Siddesh, U., Rao, C. N.R. *Phys. Rev. B*, 74(2006), 161306.
- [27] Dutta, D., Bahadur, D. *J. Mater. Chem.*, 22(2012), 24545-24551.
- [28] Kaspar, T. C., Heald, S. M., Wang, C. M., Bryan, J. D., Droubay, T., Shutthanandan, S., McCready, D.E., Kellock, A. J., Gamelin, D. R. et al. *Phys. Rev. Lett.*, 95(2005), 217203.



- [29] C. B. Fitzgerald, M. Venkatesan, A. P. Douvalis, S. Huber, J. M. D. Coey, and T. Bakas, *J. Appl. Phys.* 95 (2004), 7390.
- [30] K. Gopinadhan, Subhash C. Kashyap, Dinesh K. Pandya, and Sujeet Chaudhary, *J. Appl. Phys.* 102(2007), 113513.
- [31] J.I. Pankove, *Opt. Process.Semicond.*, Prentice- Hall. Inc., New jersey,(1971), 34.
- [32] H.X.yang, J.f. Qian, Z. X. chen, X.P. Ai, Y.u.l. Cao. *J. Phys. Chem. C* 111 (2007), 14067-14071.
- [33] Khare, Ankur, Wills, Andrew W., Ammerman, Lauren M., Noris, David J., and Aydil, Eray S. " Size control and quantum confinement in $\text{Cu}_2\text{ZnSnS}_4$ nanocrystals " *Chem. Commun.* 47 (2011), 42- 47.
- [34] M. Fong, X. T. Zu, Z. J. Li, S.Zhu, C. M. Liu, L. M. Wang, F. Gao, *Journal of Materials Science: Materials in Electronics* 19, 8 (2008), 868-874.
- [35] NurulSyahidahSabri, MohdSallehMohdDeni, AzlanZakari Mahesh KumarTalari, *Physics Procedia* 25 (2012),233 – 239.

